Advanced Building Blocks in Thick Silicon on Insulator Technology: Echelle Grating Multiplexers and Reflective Multimode Interference Couplers

P. Muñoz[1,2], **J. D. Doménech**[2], **J. S. Fandiño**[1], **R. Baños**[1], **and B. Gargallo**[1]

[1]Universitat Politécnica de Valéncia, Spain
[2]VLC Photonics S.L., Spain

Abstract— In this paper we present the design, fabrication and experimental demonstration of advanced building blocks in a thick Silicon generic photonic integration platform. The platform provides a fabrication process with waveguides of different contrast ratio, through different etch levels, and the possibility of metalization in selected areas. Combining waveguiding and metals we report on Echelle Gratings (EG) multiplexers and reflective Multimode Interference (R-MMI) couplers. Several devices were designed in the same reticle and several dies were supplied by the fabrication platform. The experimental results for the individual devices are reported, as well as a die to die comparison and statistical analysis.

1. INTRODUCTION

Generic photonic integration, since its inception by 2007 [1], is becoming a foundry model for photonics, providing Multi-Project Wafers (MPWs), where users share the area of wafer, and fabrication costs. Being the technology not devoted to specific purposes, it may well serve different application domains, while the manufacturing is done in a common process. Several generic integration platforms have emerged for different photonic technologies, or material systems, and operate nowadays [2]. Very recently the Silicon-on-Insulator (SOI) platform ePIXfab, which traditionally provided Silicon technology with nanometric waveguides, of typical cross-section $W \times H$ $450 \times 220\,\text{nm}^2$, has incorporated micrometric size Silicon waveguides [3], despite this thick Silicon technology is well known and exists since long time ago [4]. In fact, thick Si is the core technology, of several market players since 2006, but using proprietary processes [5]. Demonstrating the versatility of the generic process is key, and this is achieved by developing different photonic building blocks. Thin Si photonics, Indium Phosphide and Silicon Nitride have demonstrated a wide list of building blocks [2], ranging from passive waveguide and coupling components, through filters to active blocks as modulators, amplifiers, lasers and detectors. In generic thick Si technology the basic waveguiding and coupling components have been demonstrated [6]. However, key devices as wavelength multiplexers have not been reported yet. It is widely accepted that on-chip silicon multiplexers are central to a huge number of applications [7]. Among them, the Echelle Diffraction Grating, or Echelle Grating (EG) is recognized as the multiplexing block having smallest footprint and robustness in a wide number of applications [8] compared to other alternatives such as the Arrayed Waveguide Grating [9]. In particular, in thick Si technology where the bend radius is larger than for the thin Si nanometric waveguides, the EG proves to be very convenient. Hence, the purpose of this paper is to report on EG multiplexers using metal mirrors in a generic thick Silicon manufacturing platform. The paper is structured as follows. Section 2 provides a general review of the most relevant works addressing EGs in SOI technology. Next, Section 3 reports on the experimental outcomes of the demonstrated devices, including statistical analysis of passband features such as insertion loss, polarization dependent loss (PDL), polarization dependent wavelength shift (PDWS), bandwidth, adjacent and non-adjacent cross-talk and the comparison between devices with and without metal reflectors for both polarizations. Finally, the conclusions are presented in Section 4.

2. STATE OF THE ART AND DESIGN

A summary of devices previously reported in journals is given in Table 1. For completeness, the table includes both thick and thin Si waveguide devices. The former have a typical cross-section of $3 \times 3\,\mu\text{m}^2$, and the latter typically $0.45 \times 0.22\,\text{nm}^2$. Hence, the micrometric waveguide supports both TE and TM, whereas the nanometric mainly guides TE polarization with such a cross-section. The thin Si devices have been reported for the optical telecommunication C-band (1530–1565 nm). For thick Si devices, the EG reported in [10] is an S-C band multiplexing device for passive optical networks, whereas the one demonstrated in [8] operates at S, C and L-band as well. Regarding the

Table 1: Comparison of this work with other state of the art — journal publications — (Abbreviations: PDL, Polarization Dependent Loss; PDWS, Polarization Dependent Wavelength Shift; FSR, Free Spectral Range; n.a. does not apply; — not available; * bands may not be covered in full; † 4 channel devices with and without metalized grating lines fabricated for comparison, all the figures reported in this column are for metalized devices; ††SiO_2 256 nm layer and 150 nm layer of Al; DBR, Distributed Bragg Reflector).

	This work†	[8]	[10]	[11]	[12]	[13]
Technology	Thick Si	Thick Si	Thick Si	Thin Si	Thin Si	Thin Si
Waveguide	$3.00 \times 3.00\ \mu m^2$	$3.00 \times 3.00\ \mu m^2$	$3.00 \times 3.00\ \mu m^2$	$0.45 \times 0.22\ \mu m^2$	$0.50 \times 0.22\ \mu m^2$	$0.45 \times 0.22\ \mu m^2$
Polarization (s)	TE+TMTE+TM	TE+TM	TE	TE	TE	
Operation*	S, C, L bands	S, C, L band	S,C bands	C-Band	C-Band	C-band
Grating Facet	SiO_2-Al/None††	Al (150 nm)	-	DBR	45 corner cube	None
# channels	4	12	2	30	-	4
focal length	275 µm	-	-	-	-	-
spacing	20 nm 8 nm	70 nm	3.2 nm	3.2 nm	20 nm	
FSR	198 nm	-	-	-	-	-
Order	8	-	-	-	20	-
Grating length	250 µm	-	-	-	-	135 µm
Grating period	5.425 µm	-	-	-	-	4.35 µm
# grooves	46	-	-	-	38	31
Passband	Gauss	Flat	Flat	Gauss	Gauss	Gauss
Results						
Insertion loss	5.68±0.32 dB	1.7 dB	1.8 dB	3 dB	3 dB	7.5 dB
Loss uniformity	3.84±0.90 dB	-	-	4 dB	0.5 dB	0.6 dB
PDL	0.58±0.44 dB	0.2 dB	0.2 dB	n.a.	n.a.	n.a.
PDWS	0.32±0.74 nm	0.3 nm	0.3 nm	n.a.	n.a.	n.a.
BW 1 dB	4.18±1.12 nm	5.5 nm	-	-	-	-
BW 3 dB	7.30±1.32 nm	-	20 nm	-	-	-
BW 10 dB	12.54±1.20 nm	-	-	-	-	-
BW 20 dB	16.11±1.06 nm	-	-	-	-	-
Adjacent Xt	−34.14±2.71 dB	−25 dB	−32 dB	−15 dB	−19 dB	−30 dB
Non-adjacent Xt	−38.33±3.23 dB	-	-	−25 dB	-	-
Footprint	$0.12\ mm^2$	$15.75\ mm^2$	$3.24\ mm^2$	$0.5\ mm^2$	$0.05\ mm^2$	$0.04\ mm^2$

grating line, some of them report different techniques to increase the reflectivity, to compensate, up to some extent, the Fresnel reflection loss [14] taking place between the Si guiding layer, and the cover layer, in some cases just air, in others SiO_2. Hence, Distributed Bragg Reflectors (DBR) [11], a 45 corner cube [12] and the deposition of metals as aluminum [8] have been reported. The latter requires additional processing steps, but the achieved reflectivity may be larger than the other techniques, albeit the former are attained within the same waveguide lithography. EGs with 4 channels were designed according to the specifications in the first two columns of Table 1. The design process is as reported in [15]. The devices are based on a curved facet type grating and make use of input/output waveguides with the following characteristics: width 2.4 µm, side etching 1.75 µm, input waveguides center at 36° and output waveguides center at 41°. The slab mode effective and group indices were computed to be 3.46 and 3.6 respectively. In the design area, two EG devices, with and without metalization, were included.

3. EXPERIMENTAL RESULTS

3.1. Fabrication and Characterization

The devices were fabricated in the generic technology platform provided by VTT Finland [6]. The typical performance for 3 µm width waveguides is: propagation loss 0.1 dB/cm, fiber i/o coupling up to 90% (lensed fibers), or 40% (regular fiber) and small polarization dependence [3]. Additional metalization steps are available in the platform, and they were employed to cover some of the grating lines in our devices. To be precise, the mirrors are formed by depositing two thin layers on top of the Silicon guiding layer: a first layer of SiO_2 (265 nm, corresponding to a quarter-wave), and a second layer of 150 nm aluminum. A cross-section of the aluminium mirror layer stack is shown in Figure 1(a). As reported by the manufacturers, reflectivity of these combined layers can be as good as 92.7% [16]. Nonetheless we employed other reflective devices within the same dies [17] based on Multimode interference reflectors (MIRs). Figures 1(b) and (c) show a schematic 3D representation of a 2-port MIR, as well as an SEM picture of a fabricated device, respectively. To assess on the MIR reflectivity, Fabry-Pérot test structures made of a concatenation of two MIRs were employed to extract the wavelength dependent reflectivity. Figure 2(a) shows an schematic diagram of the test structures, while Figure 2(b) is an SEM picture of a fabricated device. The two MIRs form an integrated resonant cavity with a periodic spectrum made of interference fringes. The depth of these fringes, also known as the extinction ratio (ER), depends on the total effective reflectivity of the MIR under test. As shown in Figure 2(c), our conclusion is the reflectivity in these chips is approximately 79.4 %. Full details can be found in [17]. Finally, a SEM micrograph of the EG devices is shown in Figure 1(d), with an inset showing the view of the grating line, where the metal area is highlighted in pseudo-color. During the measurements the chips of were held on

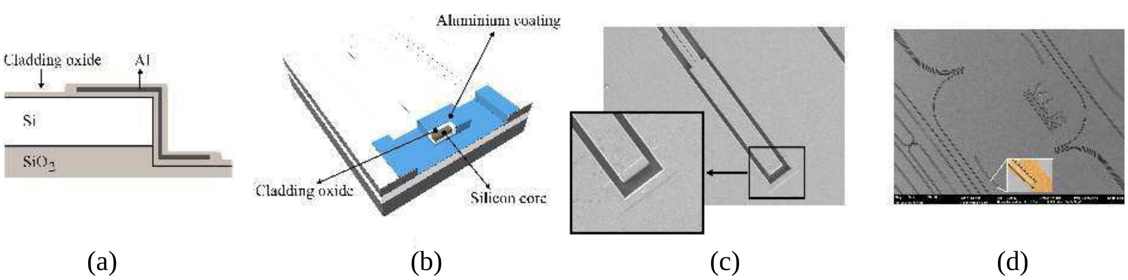

Figure 1: (a) Cross-section of the aluminium mirror layer stack. (b) 3D Model of a 2-port MIR with aluminium mirror. (c) SEM picture of a fabricated device. (d) SEM micrographs of fabricated devices, EG device, inset with detail of the grating line (metalization in pseudo-color).

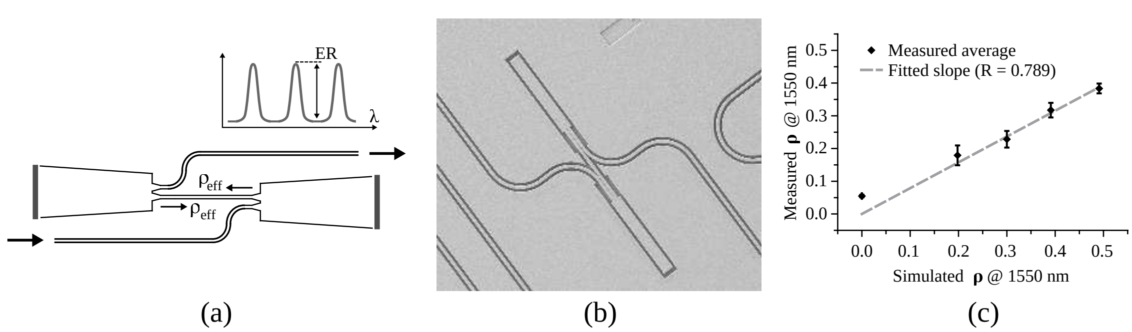

Figure 2: (a) Schematic diagram of the structures employed to measure the effective reflectivities of the devices under test. (b) SEM picture of a test structure. (c) Measured average and standard deviations of the reflectivities versus the simulated values at 1550 nm. Grey dashed line: Slope fitted to the data that provides an estimate of the average intrinsic losses both in the mirror and in the access waveguides.

top of a thermally controlled (25°C) vacuum chuck. The in/out coupling stages consists of a fiber holder, collimating lens, free space polarizer and microscope objective.

3.2. Transmission Spectra

The transmission spectra of the EG is shown in Figure 3(a). The results are normalized with respect to a straight (test structure) waveguide. The minimum insertion loss for the EG is around 5 dB, and the loss non uniformity is around 1 dB. The graph also shows the overlaid spectra for TE and TM polarizations, which were set using bulk filters in the in coupling stages mentioned previously. In accordance to the small polarization dependence of this thick Si technology, from the graphs low PDL and PDWS are observed. For these particular devices PDL is as low as 0.2 dB, except for the third channel on Figure 3(a), and PDWS is as low as 0.3 nm. Both values are in good agreement with other reported thick Si EGs [8, 10]. Finally, and less noticeable, all the passbands have a common feature, that is a small side lobe close to the left side of the main lobe (towards shorter wavelengths). This side lobe is also predicted in the design and simulation stage, where slanted grating sidewall (between 1–2°) were included. The slanted grating walls result into slightly increased insertion loss in the main band, due to the coupling to higher order (vertical) slab modes in the EG, which in turn result into the aforementioned left side lobe present in all the spectral traces [8].

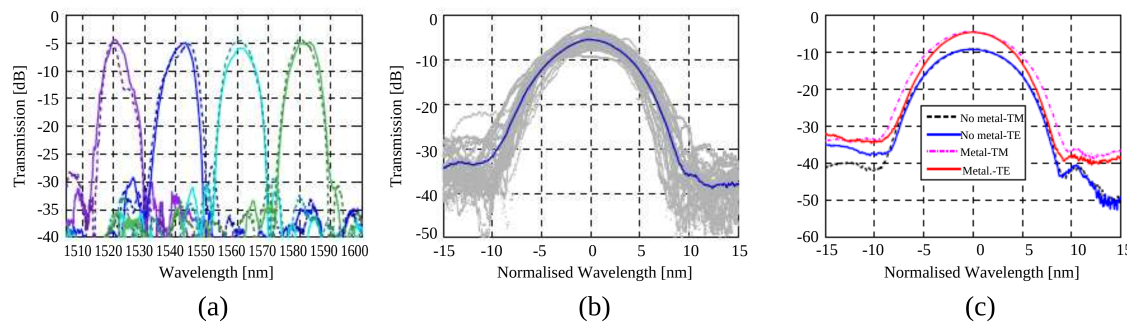

Figure 3: Transmission spectra for the EG with metal reflector. (a) Solid and dashed lines correspond to TE and TM polarization respectively. (b) Superimposed transmission spectra for all the devices and channels. Grey dots show the overlaid spectra for all measured channels from 5 chips, 1 device per chip. All the channels have been aligned to the same center wavelength. The blue line shows the average response. TE polarization, TM polarization exhibited similar performance. (c) Comparison of averaged responses from all the channels, with and without grating line metalization, and for TE and TM polarizations.

3.3. Passband Features Analysis

Several dies were retained for full measurements, having as target the analysis of variations among them. Each die includes test structures and two EGs, with and without metal mirrors. Devices from five dies were measured in full. Other dies were discarded due to randomly damaged i/o waveguide facets. The results shown onwards are only for TE polarization for the sake of clarity, since for TM similar results were obtained. Figure 3(b) shows the superimposed tranmission spectra for all the channels, aligned to 3-dB bandwidth center wavelength. The collected statistical features from the passbands are summarized in the first column of Table 1. Note that a part of all the variations reported for the figures related to optical power (insertion loss, loss non-uniformity, and PDL) may be attributed to different facet condition for the different EG input/output waveguides, and that they may be reduced by facet polishing [18]. In terms of channel insertion loss, the average of the peak insertion loss for all channels and dies was calculated. The EG exhibits 5.7 dB with little variations, as detailed in the table. Compared to previous reported values, Table 1 [8, 10], these are 2–4 dB larger. This maybe attributed to a non-optimized generic process which was also used for the first time to this purpose, compared to the industrial dedicated process from [8, 10]. Next, the loss uniformity of the devices was calculated as the difference between the maximum and minimum peak transmission for each device. The mean and standard deviation over all the dies is also shown in Table 1, where an average uniformity around 3.7 dB with variations of around ±1 dB. The PDL was calculated as the difference of the peak amplitude for TE and TM polarization of a given channel. The average PDL is close to 0.6 dB, whereas other thick Si references, Table 1 [8, 10] reported a PDL of 0.2 dB. In terms of PDWS, computed as the difference between the wavelengths were the

TE and TM maxima per channel are locateld, our results are on average close to those previously reported of 0.3 nm. The bandwidth was calculated from the measurements for all the devices and channels, and the obtained bandwidth values were averaged over all the channels and samples as well. The N-dB bandwidth was calculated as the wavelength difference between the two poins in the passband N-dB under the maximum. The average and standard deviation interval are given in Table 1. A Gaussian power transfer function was fitted to the 3-dB bandwidth, and the band pass fit is good down the 10-dB point from the maximum. The cross-talk was computed as the maximum value of the adjacent (non-adjacent) channel(s) in a given channel 3-dB clear window [18]. The average for adjacent channel cross-talk is around −33 dB. This is slightly better than reference [8] and similar to reference [10]. The non-adjacent channel cross-talk is approximately −38 dB.

3.4. Echelle Gratings with Metal Mirrors Analysis

Figure 3(c) shows the averaged spectra for all channels and chips. The difference for the metalized and non-metalized devices is 4.62 dB and 4.67 dB for TE and TM. In all the cases, both devices (with and without mirror) sit on the same die, that is the grating line patterning is expected to be similar, despite the orientation is different, as can be seen in Figure 1(d). In an ideal situation, one would expect the loss difference between devices with and without mirrors to be close to the Fresnel reflection loss. Since the difference between the incident (input waveguide) and diffraction (output waveguides) angles is 5°, the Fresnel reflection loss contribution is calculated to be 7.83 dB for TE, and 7.51 dB for TM. Using the mirror structure described above, ideally the loss in the interface would 0.069 dB and 0.064 dB for TE and TM respectively, slightly less lossy for TM [17]. Nonetheless we measured these SiO_2-Al mirrors reflectors in the dies provide a reflectivity in average of 79.4% (1.0 dB loss) [17]. Hence, this approximately 2.0 dB variations, which may be attributed, besides to poorer performance of the mirrors in some cases, to different sources of errors: different imperfections in the grating lines of metalized and non metalized devices (roughness, rounded corners, ...) as well as differences in the in/out coupling properties of the different samples used to average and substract.

4. CONCLUSION AND OUTLOOK

In this paper we reported on Echelle Gratings multiplexers equipped with metal mirrors, designed and manufactured using thick Silicon photonic integration technology. Multimode interference reflectors were also designed and demonstrated, from which the reflectivity of the metal layers was derived. The paper supplies information of variations on different figures of merit for the multiplexers. Furthermore, the comparison between devices with and without metal mirrors is supplied as well, for different polarizations.

ACKNOWLEDGMENT

The authors acknowledge financial support by the Spanish CDTI NEOTEC start-up programme, the Spanish MINECO project TEC2013-42332-P, acronym PIC4ESP, project FEDER UPVOV 10-3E-492 and project FEDER UPVOV 08-3E-008. B. Gargallo acknowledges financial support through FPI grant BES-2011-046100. J. S. Fandiño acknowledge financial support through FPU grant AP2010-1595.

REFERENCES

1. "Towards a foundry model for micro- and nanophotonic ics," *European Network of Excellence on Photonic Integrated Components and Circuits*, Mar. 2007.
2. Munoz, P., J. Domenech, et al., "Evolution of fabless generic photonic integration," *2013 15th International Conference on Transparent Optical Networks (ICTON)*, Jun. 2013.
3. Aalto, T., M. Cherchi, et al., "Launching of multi-project wafer runs in epixfab with micron-scale silicon rib waveguide technology," *Proc. SPIE*, Vol. 8990, 899003-1–899003-11, 2014.
4. Soref, R. A., "Silicon-based optoelectronics," *Proceedings of the IEEE*, Vol. 81, No. 12, 1687–1706, Dec. 1993.
5. Mounier, E. and C. Troadec, "Silicon photonics 2014," Yole Development, Tech. Rep., 2014.
6. Aalto, T., M. Cherchi, et al., "Dense photonics integration on a micron-scale SOI waveguide platform," *2013 IEEE 10th International Conference on Group IV Photonics (GFP)*, 107–108, Aug. 2013.
7. Dai, D. and J. E. Bowers, "Silicon-based on-chip multiplexing technologies and devices for peta-bit optical interconnects," *Nanophotonics*, Vol. 3, Nos. 4–5, 283–311, 2014.

8. Feng, D., W. Qian, et al., "Fabrication insensitive echelle grating in silicon-on-insulator platform," *IEEE Photonics Technology Letters*, Vol. 23, No. 5, 284–286, Mar. 2011.
9. Pathak, S., P. Dumon, et al., "Comparison of AWGs and echelle gratings for wavelength division multiplexing on silicon-on-insulator," *IEEE Photonics Journal*, Vol. 6, No. 5, 1–9, Oct. 2014.
10. Bidnyk, S., D. Feng, et al., "Silicon-on-insulator-based planar circuit for passive optical network applications," *IEEE Photonics Technology Letters*, Vol. 18, No. 22, 2392–2394, Nov. 2006.
11. Bogaerts, W., S. Selvaraja, et al., "Silicon-on-insulator spectral filters fabricated with CMOS technology," *IEEE Journal of Selected Topics in Quantum Electronics*, Vol. 16, No. 1, 33–44, Jan. 2010.
12. Horst, F., W. Green, et al., "Silicon-on-insulator echelle grating WDM demultiplexers with two stigmatic points," *IEEE Photonics Technology Letters*, Vol. 21, No. 23, 1743–1745, Dec. 2009.
13. Brouckaert, J., W. Bogaerts, et al., "Planar concave grating demultiplexer fabricated on a nanophotonic silicon-on-insulator platform," *Journal of Lightwave Technology*, Vol. 25, No. 5, 1269–1275, May 2007.
14. Saleh, B. and M. Teich, *Fundamentals of Photonics*, 2nd Edition, Chapter 6, 197–242. Wiley, 2007.
15. Lycett, R., D. Gallagher, and V. Brulis, "Perfect chirped echelle grating wavelength multiplexor: Design and optimization," *IEEE Photonics Journal*, Vol. 5, No. 2, 2400123, Apr. 2013.
16. Cherchi, M., S. Ylinen, et al., "MMI resonators based on metal mirrors and MMI mirrors: An experimental comparison," *Opt. Express*, Vol. 23, No. 5, 5982–5993, Mar. 2015.
17. Fandio, J. S., J. D. Domnech, and P. Muoz, "Two-port multimode interference reflectors based on aluminium mirrors in a thick SOI platform," *Physics Optics*, arXiv: 1504.01549, Online Available: http://arxiv.org/abs/1504.01549.
18. Piels, M., J. Bauters, et al., "Low-loss silicon nitride AWG demultiplexer heterogeneously integrated with hybrid III-V/silicon photodetectors," *Journal of Lightwave Technology*, Vol. 32, No. 4, 817–823, Feb. 2014.